Enhancing the Photon- and Gas-Sensing Properties of a Single SnO₂ Nanowire Based Nanodevice by Nanoparticle Surface Functionalization

Qin Kuang,[†,‡] Chang-Shi Lao,[‡] Zhou Li,[‡] Yu-Zi Liu,[‡] Zhao-Xiong Xie,*,[†] Lan-Sun Zheng,[†] and Zhong Lin Wang*,[‡]

State Key Laboratory for Physical Chemistry of Solid Surfaces and Department of Chemistry, College of Chemistry and Chemical Engineering, Xiamen University, Xiamen, 361005, People's Republic of China, and School of Materials Science and Engineering, Georgia Institute of Technology, Atlanta, Georgia 30332-0245

Field-effect transistors based on a single SnO₂ nanowire were successfully fabricated, and their photon- and gas-sensing properties were investigated. It is found that the sensitivity of single SnO₂ nanowire based devices was remarkably improved by surface functionalization with ZnO or NiO nanoparticles. The heterojunction between the surface coating layers and SnO₂ and the corresponding coupling effect of the two sensing materials play a critical role in controlling device sensitivity.

1. Introduction

Metal oxides such as SnO₂, ZnO, WO₃, and In₂O₃ are widely used as sensing materials in industry, such as environmental monitoring, security systems, biomedical instruments, and healthcare systems.[1–5] The general sensing mechanism of these sensors is based on the resistance change of the functional sensing elements when they are subject to different environments such as different gases, light, and humidity. One-dimensional (1D) metal oxide nanostructures based sensing devices are of great importance for significantly improving the performance of sensors built using thin film technology. Due to the excellent physical and chemical properties resulting from the reduced sizes, 1D metal oxide nanostructures like nanowires (NWs) and nanobelts (NBs) are regarded as promising candidates for use as sensing units and have drawn much attention recently. To date, a series of nanosized chemical sensors have been successfully constructed.[6–13] In comparison with traditional metal oxide sensors, these metal oxide NW or NB-based sensors exhibit many advantages, such as lower operating temperature (even at room temperature), higher sensitivity (part-per-billion and above), and better compatibility with existing microelectromechanical system (MEMS) technology.

Among all of the metal oxide sensing materials, SnO₂ is one of the most promising substances due to its high sensitivity and stability, which ensure superior performance of these devices. However, to explore the detection limit and enhance measurement accuracy is still a challenge for the SnO₂-based sensing devices. Recently, many solutions have been developed to improve the sensing performance of SnO₂-based sensors, including optimization of operation temperature,[14] surface functionalization,[9,15] doping of other additives into the SnO₂ matrix,[16,17] and incorporation of a heterojunction system.[18–21] However, most of these efforts are focused on those conventional metal oxide sensors (i.e., powder or film-based sensors) rather than the sensors based on a single 1D nanostructure. Considering the special geometrical characteristic of 1D nanostructures, the sensing performance of SnO₂ NW and NB-based

sensors has a strong dependence on their surface states. Therefore, surface functionalization is a very effective strategy for enhancing the sensitivity of the devices.

Previous work on surface functionalization has been focused on coating of transition metal catalysts (such as Au, Pt, and Pd) and other metal oxide sensing materials (such as CuO, NiO, and Sb₂O₃). The general working principle of these additives for surface functionalization can be classified into three categories: (1) introducing more structure defects in metal oxide sensing materials by diffusion of the additives; (2) accelerating the gas reaction on the metal oxide surface by catalytic action of the additives; (3) changing surface band structure of metal oxide sensing materials by the formation of heterojunctions including p−n junctions and n−n junctions. Efforts have been devoted into the improvement in sensing performance of 1D SnO₂ nanostructure based sensors according to these methods.[9,15,22] For example, Kolmakov et al. reported that gas sensitivity was enhanced by functionalizing a single SnO₂ NW/NB with Pd particles.[9] And the study of Qian et al. demonstrated that the detection limit of a single SnO₂ NB-based sensor could reach 10 ppm for CO after modification by Au nanoparticles.[22]

In this article, field-effect transistors (FET) based on single SnO₂ NW were successfully fabricated, and the corresponding photon- and gas-sensing performances were systematically investigated. It is demonstrated that the sensitivity of the device can be remarkably improved by surface functionalization with ZnO or NiO nanoparticles via magnetron sputtering. The heterojunction between the surface coating layers and SnO₂ and the corresponding coupling effect of the two sensing materials play a key role in enhancing the sensitivity. This method can work as a feasible solution to improve the selectivity of SnO₂-based sensors and accelerate the commercialization of metal oxide nanodevices.

2. Experimental Section

The SnO₂ NWs used here were synthesized by a thermal evaporation method reported in ref 23. In a typical experiment, an alumina boat loaded with 2 g of SnO₂ and graphite (molar ratio 1:4) mixed powder was placed in the middle of a horizontal tube furnace. And then the system was heated to 1000 °C for 2 h with Ar gas at a flow rate of 50 sccm and a pressure of 200

* Corresponding authors. E-mail: zxxie@xmu.edu.cn (Z.-X.X.), Zhong.
wang@mse.gatech.edu (Z.-L.W.).
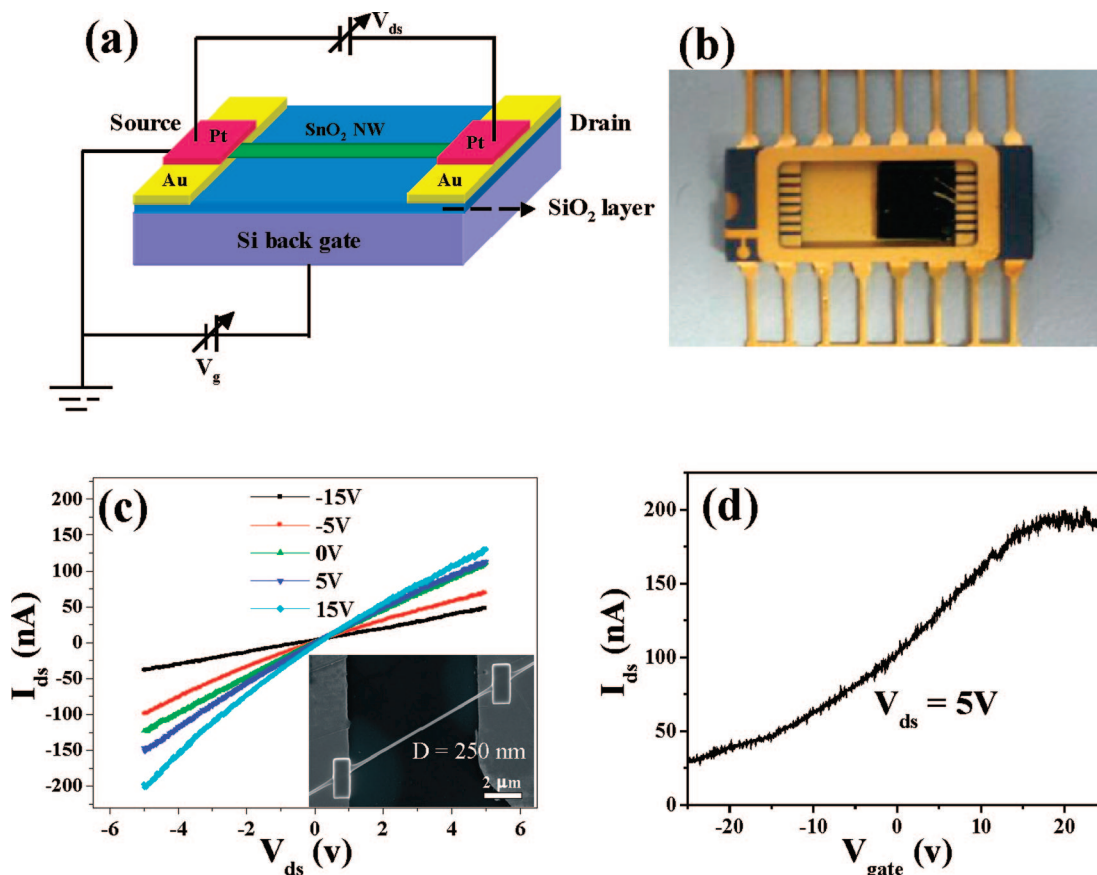† Xiamen University.
‡ Georgia Institute of Technology.

Figure 1. (a) Schematic illustration of a single SnO_2 NW-based FET. (b) A single SnO_2 NW-based FET packed in a chip. (c) Output characteristic curves (i.e., gate-dependent $I-V$ curves) and (d) transfer characteristic curve (i.e., $I-V_{gate}$ curve) of the single SnO_2 NW-FET recorded at room temperature. The inset in (c) is a corresponding SEM image of the single SnO_2 NW.

Torr. The as-synthesized SnO_2 NWs were then collected and dispersed in ethanol. The devices were fabricated by transferring the NWs onto a silicon substrate with predefined Au electrodes. In this way, the NW was lying across the Au electrodes. Then, a 500 nm thick Pt layer was deposited on the contact point of the SnO_2 NW and Au electrode by focused ion beam (FIB) deposition to enhance the contacts. Surface functionalization of SnO_2 NWs was carried out in a magnetron sputtering system. The average sizes of ZnO particles and NiO particles deposited on the surface of single SnO_2 NWs were 10 and 2 nm, respectively. Scanning electron microscopy (SEM), transmission electron microscopy (TEM), and energy dispersive X-ray spectroscopy (EDS) were used to characterize the structures and composition of SnO_2 NWs after deposition of NiO and ZnO. It should be noted that the characterization studies before and after surface functionalization were carried out on the same SnO_2 NW, which eliminated the variation in properties in different NW samples.

3. Results and Discussion

3.1. Field-Effect Transistor Properties of a Single SnO_2 NW-Based Nanodevice. Figure 1a is a schematic illustration of a single SnO_2 NW-based FET, in which two metal leads are used as source and drain electrodes, the silicon substrate acts as the back gate, and a 300 nm thick SiO_2 serves as the insulating gate dielectric layer. As shown in Figure 1b, the single SnO_2 NW-based FET was packed in a chip by wire bonding. In Figure 1c are typical output characteristic curves obtained from the nanodevice at different V_g from -15 to $+15$ V. The linear $I-V_{ds}$ curves indicate that the SnO_2 NW has an ohmic

contact with metal electrodes. Figure 1d is a typical transfer characteristic curve obtained from the device at V_{ds} of 5 V. It is found that the conductance (i.e., I_{gate}) of the single SnO_2 NW increases with a sweeping positive gate voltage (i.e., V_g) from -25 to $+25$ V. The transport characteristics show the performance of a typical n-type depletion metal oxide FET. From the transfer characteristic curve, transconductance ($g_m = \partial I_{ds}/\partial V_g$) of this single SnO_2 NW-based FET is calculated to be 6.0 nS and the effective field-effect carrier mobility (μ_e) is also estimated to be 30 cm^2/V·S according to $g_m = \mu_e V_{ds}CZ/L$ where L is the channel length, Z is the channel width, and C is the oxide capacitance per unit area.[24]

3.2. Enhancing Sensing Properties of a Single SnO_2 NW-Based Nanodevice by ZnO Nanoparticle Surface Functionalization. As discussed previously, surface functionalization is an effective method in improving the device performance. We first present the effect of surface functionalization on the electrical properties of the NW. ZnO nanoparticles with about 10 nm in thickness were deposited on the surface of SnO_2 NWs via magnetron sputtering (see the inset of Figure 2a). Figure 2a shows typical $I-V$ curves of the single SnO_2 NW-based device before and after ZnO deposition at air and room temperature. From this figure, it is found that surface functionalization with ZnO nanoparticles can largely increase the conductivity of SnO_2. According to our calculation, the resistance (2.86×10^6 Ω) of ZnO-functionalized SnO_2 NW is only $1/10$ of that (2.83×10^7 Ω) of SnO_2 NW without functionalization. The increase in the conductance should originate from the change of surface structure and defects in SnO_2 NWs. In the deposition process, the bombardment caused by ZnO deposition produces high-
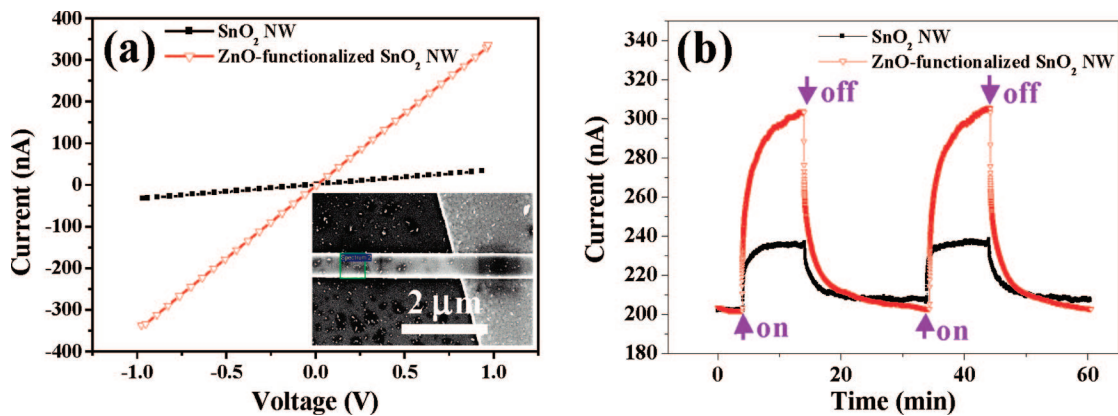
Sensing Performance of a Single SnO₂ NW-Based FET

J. Phys. Chem. C, Vol. 112, No. 30, 2008 **11541**

Figure 2. (a) $I-V$ curves of the single SnO₂ NW-based device before and after ZnO deposition. The inset is the corresponding SEM image of the single SnO₂ NW device after ZnO deposition. The deposition thickness of ZnO is about 10 nm. (b) Photoconductance response curves of the single SnO₂ NW-based sensor before and after surface functionalization with ZnO nanoparticles. The wavelength of UV light in our studies is 365 nm.

density oxygen vacancies on the surface of SnO₂ NWs. The increase of structure defects will inevitably bring an important influence on photoelectrical properties such as photoconductance and gas sensing of the device.

Figure 2b shows two photoconductance response curves of the SnO₂ NW before and after surface functionalization with ZnO nanoparticles. The measurements show that when the SnO₂ NW was exposed to UV light, the current abruptly increased and reached a steady value, and when UV light was shut off, the current gradually recovered to the initial value. It is worth mentioning that the response sensitivity ($S = R_{dark}/R_{uv}$) of the single SnO₂ NW functionalized with ZnO nanoparticles is 1.50, which is almost 2 times higher than that of the initial SnO₂ NW-based sensor. Such significant enhancement in photoconductance achieved surface functionalization is an interesting phenomenon. This is probably the first report about the enhancement in photoconductance by integrating ZnO and SnO₂, although extensive studies have been carried out separately for ZnO and SnO₂ 1D nanostructures.[6,7,25]

Previous studies have proved that the photoconductance of metal oxides like ZnO and SnO₂ involves two processes including adsorption/desorption of oxygen species and electron transitions excited by photons.[6] Hole−electron pairs in the metal oxide are generated under the illumination of UV light. The photon-generated holes will be pulled to the surface by the electric field and recombine with the adsorbed oxygen species (O_2^- and O_2^{2-}). At the same time, the photon-generated electrons remain as free carriers and consequently enhance the conductance of the NW. The electron−hole generation is closely related to the wavelength of the exciting light.[26,27] According to the equation $\lambda = hc/E_g$ (h, Planck constant; c, light velocity; E_g, band gap of metal oxide semiconductor), electron−hole pairs can only be generated when the wavelength of exciting light is shorter than the limit of the permissible exciting wavelength. For SnO₂ with the band gap energy of 3.60 eV, theoretically the intrinsic photoconductance could not be excited by the UV light of 365 nm, but the pure SnO₂ NW shows a weak photon-sensing response under UV light in the present experimental conditions. This weak photon-sensing response should be accounted for by an extrinsic photoconductance of SnO₂ resulting from extrinsic electron transition between some impurity and defects states. Due to a fast recombination of the photon-generated electron−hole pairs, this extrinsic photoconductance of SnO₂ is very weak compared with its intrinsic photoconductance. When the surface of the single SnO₂ NW is coated with ZnO nanoparticles, both the intrinsic photoconduc-

tance of ZnO and the extrinsic photoconductance of SnO₂ can be excited by the UV light of 365 nm at the same time, and a more important point is that a charge separation process takes place between ZnO and SnO₂ due to the difference of their energy gaps and misalignment of the energy bands. The conductance band energy of SnO₂ is lower than that of ZnO by 0.7 eV so that the SnO₂ can act as an acceptor for photon-generated electrons in ZnO-functionalized SnO₂ NWs, whereas the photon-generated holes in SnO₂ tend to be trapped within the ZnO particle. The charge separation of photon-generated electrons and holes greatly reduces their recombination probability and accordingly enhances the photoconductance of ZnO-functionalized SnO₂ NWs. Such charge separation principle has been used to account for the photocatalytic properties of ZnO−SnO₂ coupled oxide nanoparticles.[28,29] The similar strategy to increase the photon-sensing properties via surface functionalization has been applied in our previous study of the single ZnO NB-based UV detector where the UV response of the ZnO NB was enhanced by up to 5 orders of magnitude with surface coating of different polymers.[7]

The gas-sensing properties of these SnO₂ NWs after surface functionalization were also investigated. Figure 3a shows gas-sensing sensitivities of a SnO₂ NW-based sensor before and after ZnO surface coating to three detected gases. The gases tested are 500 ppm H₂S, CO, and CH₄ at an operation temperature of 250 °C. It is found that the changes on the sensitivity ($S = R_{N2}/R_{gas}$) of the SnO₂ NW after ZnO surface coating behave distinctively for different gases. For H₂S, the sensitivity of the device increased from 1.26 to 1.50, but in contrast, the sensitivity to CO decreased from 1.15 to 1.08. The sensitivity of the device to CH₄ was just slightly affected by the coated ZnO. From the experimental results, selectivity of the single SnO₂ NW was improved to a certain extent by surface functionalization. Figure 3b shows the different sensitivity to three detected gases of the ZnO-functionalized SnO₂ NW-based sensor at different operation temperatures, which indicates that the device has the highest sensitivity to H₂S at 350 °C and to CH₄ at 450 °C. By combining ZnO surface functionalization and choosing the optimistic operation temperature, the sensitivity and selectivity of the device can be effectively improved.

As far as gas-sensing properties are concerned, the working mechanisms of SnO₂ and ZnO are very similar. Both of them are typical surface-controlled gas-sensing materials. Many studies have demonstrated that ZnO−SnO₂ composite based sensors possess a better selectivity to some special gases such as C₂H₅OH and H₂S. Possible mechanisms for selective
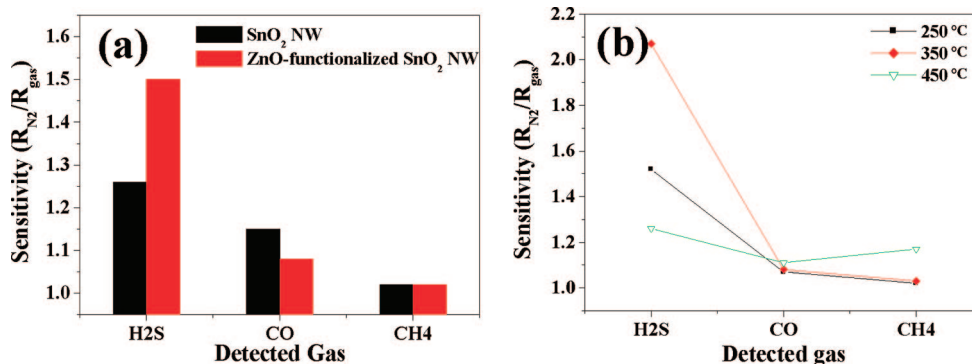
Figure 3. (a) Comparison of gas-sensing sensitivity of the pure and ZnO-functionalized SnO_2 NW-based sensor to three detected gases. (b) Sensitivity to three detected gases of the ZnO-functionalized SnO_2 NW-based sensor at different operation temperatures. The concentration of detected gases is 500 ppm, the operation temperature is 250 °C, and the fixed bias is 1 V.
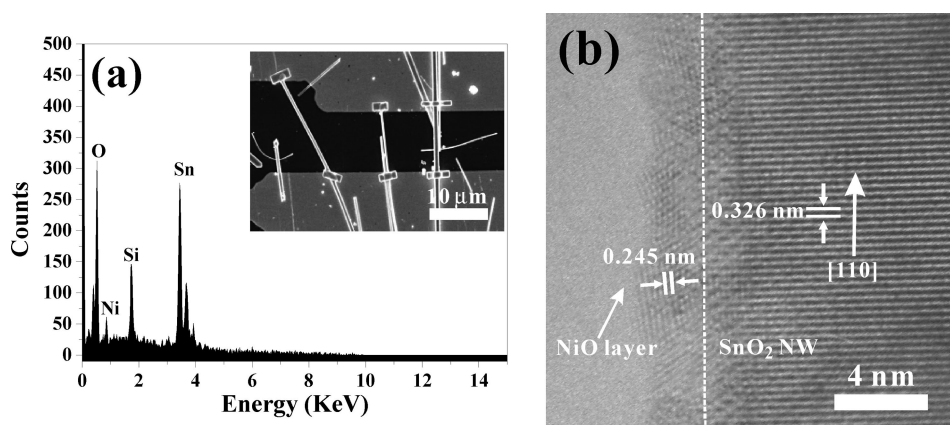

Figure 4. (a) EDS spectrum and (b) typical high-resolution TEM image of a NiO-functionalized SnO_2 NW. The inset in (a) is the corresponding SEM image of the single NiO-functionalized SnO_2 NW device. The deposition thickness of NiO is about 2 nm.

enhancement of ZnO−SnO_2 composite structure have been proposed.[20,30–34] It is suggested that some intermediate compounds such as Zn_2SnO_4 and $ZnSnO_3$ may form during the sintering process at high temperature (600 ∼ 800 °C) and act as highly selective sensing elements to C_2H_5OH and NO_2.[30,31] However, our operation temperature is in the range of 250 ∼ 450 °C. And no secondary phases were found in the XRD spectrum. Therefore, this mechanism is not responsible for the improvement in the selectivity of ZnO-functionalized SnO_2 NW. Another possible mechanism may be the formation of n−n heterojunction with an energy difference of about 0.75 eV between ZnO and SnO_2.[20] The heterojunction contains two sensing materials with two different reductive−oxidative and acid−base properties. The adsorption/desorption and oxidation/reduction processes of the detected gas might be greatly promoted by the heterojunction, although more studies will be needed to determine the detailed sensing mechanism.

3.3. Enhancing Sensing Properties of a Single SnO_2 NW-Based Nanodevice by NiO Nanoparticle Surface Functionalization. The influence on the gas-sensing properties of SnO_2 NW from NiO surface functionalization is also investigated in a similar procedure. A layer of NiO with 2 nm thickness was deposited on the surface of a SnO_2 NW via magnetron sputtering. The inset of Figure 4a is a typical SEM image of the device after NiO deposition. Although no visible particles are found from the SEM image, the corresponding EDS spectrum (Figure 4a) clearly shows the presence of elemental Ni. The direct evidence of NiO deposited on the SnO_2 NW surface is provided by high-resolution TEM characterization. As shown in Figure 4b, the single-crystalline SnO_2 NW grows along the [110] direction and its surface is coated with a thin

layer of NiO film consisting of numerous nanoparticles. Although the interface area (the dashed line in Figure 4b) seems to be amorphous, the discontinuous layer exhibit clear lattice fringes with a spacing of about 0.245 nm, which is consistent with that of {111} planes of cubic NiO (JCPDS 04-0835). It is well-known that NiO is not only an excellent catalyst but also a good p-type sensing material.[35–37] Therefore, the presence of the NiO layer on the surface may enhance the gas-sensing properties of the single SnO_2 NW-based sensors.

Figure 5a shows the response curves of the pure and NiO-functionalized SnO_2 NW to CO and CH_4 with concentrations of 100 ∼ 500 ppm. The response sensitivity of SnO_2 NWs has a good reproducibility for the same concentration of detected gas. Furthermore, the response is proportional to the concentration of the detected gas. The corresponding concentration-dependent sensitivity curves are shown in Figure 5b. We find that there is a large difference in sensitivity for two detected gases (CO and CH_4) of pure SnO_2 NW without NiO coating. For the 500 ppm concentration, the sensitivity to CO is up to 9.8, whereas the sensitivity to CH_4 is only 3.3. After NiO surface functionalization, the sensitivity of SnO_2 NW to CO is magnified to 15.9, whereas the sensitivity of SnO_2 NW to CH_4 is not obviously affected. These results prove that the selectivity to CO and CH_4 of the device can be greatly improved by NiO surface functionalization.

The formation of NiO film on the NW surface might be responsible for the improvement on selectivity of the single SnO_2 NW-based device. In previous similar studies, some possible mechanisms based on the p−n heterocontact were proposed to explain the improvement in the selectivity of composite metal oxide sensors including CuO−ZnO, CuO−
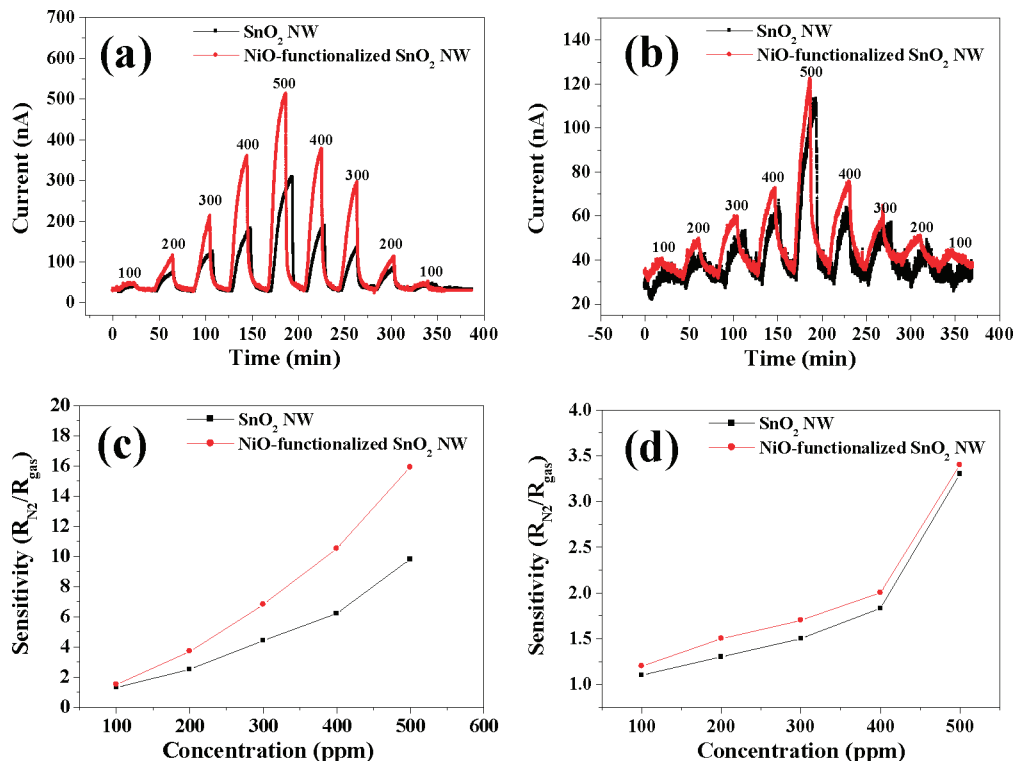
Sensing Performance of a Single SnO$_2$ NW-Based FET

J. Phys. Chem. C, Vol. 112, No. 30, 2008 **11543**

Figure 5. Gas-sensing response curves and corresponding concentration-dependent sensitivity curves of the pure and NiO-functionalized SnO$_2$ NW-based sensor to (a and c) CO and (b and d) CH$_4$. The concentration of detected gases is from 100 to 500 ppm, and the operation temperature is 250 °C.

SnO$_2$, and NiO−SnO$_2$.[20,38–43] According to the mechanism proposed by Hidalgo et al.[42] adsorbed CO on the NiO surface would react with adsorbed oxygen on the SnO$_2$ surface, and hence, the sensitivity of the metal oxide sensor should depend upon the catalytic activity for CO oxidation. In addition, the NiO layer might be reduced into Ni particles that would increase the conductance of the SnO$_2$ sensing elements. Although there is still a debate on the function of the p−n heterojunction in the improvement of selectivity up to now, it has been verified that the coordinate effect of two sensing centers of NiO and ZnO plays a key role.

4. Conclusions

In summary, we have successfully fabricated an FET based on a single SnO$_2$ NW and acquired useful information about the electron transport of the nanodevice. In addition, we achieved the improvement of photon- and gas-sensing properties of the devices by deposition of ZnO or NiO nanoparticles on the surface of the SnO$_2$ NW. Some possible mechanisms based on the heterojunction (i.e., n−n junction for ZnO−SnO$_2$ and p−n junction for NiO−SnO$_2$) and corresponding coordinate effect of two sensing centers are proposed to explain the function of these surface additives. Besides heterojunctions, many other factors, such as the size and crystalline state of surface additives and the concentration change of structure defects in the NW, may bring a pronounced influence on the photon- and gas-sensing performance of the SnO$_2$ NW-based device. Therefore, it is difficult to use a uniform model to completely elucidate the nature of the surface additives. Despite this, surface functionalization is a good strategy to improve the sensitivity and selectivity of the SnO$_2$-based nanodevice and breaks a promising path to eventually achieve the practicability of metal oxide nanodevices.

References and Notes

(1) Ansari, S. G.; Boroojerdian, P.; Sainkar, S. R.; Karekar, R. N.; Aiyer, R. C.; Kulkarni, S. K. *Thin Solid Film* **1997**, *295*, 271–276.

(2) Nayral, C.; Ould-Ely, T.; Maisonnat, A.; Chaudret, B.; Fau, P.; Lescouzeres, L.; Peyre-Lavigne, A. *Adv. Mater.* **1999**, *11*, 61–63.

(3) Martins, R.; Fortunato, E.; Nunes, P.; Ferreira, I.; Marques, A.; Bender, M.; Katsarakis, N.; Cimalla, V.; Kiriakidis, G. *J. Appl. Phys.* **1996**, *96*, 1398.

(4) Solis, J. L.; Heel, A.; Kish, L. B.; Granqvist, C. G.; Saukko, S.; Lantto, V. *J. Am. Ceram. Soc.* **2001**, *84*, 1504–1508.

(5) Gurlo, A.; Ivanovskaya, M.; Barsan, N.; Schweizer-Berberich, M.; Weimar, U.; Gopel, W.; Dieguez, A. *Sens. Actuators, B* **1997**, *44*, 327–333.

(6) Soci, C.; Zhang, A.; Xiang, B.; Dayeh, S. A.; Aplin, D. P. R.; Park, J.; Bao, X. Y.; Lo, Y. H.; Wang, D. *Nano Lett.* **2007**, *7*, 1003–1009.

(7) Lao, C. S.; Park, M. C.; Kuang, Q.; Deng, Y. L.; Sood, A. K.; Polla, D.; Wang, Z. L. *J. Am. Chem. Soc.* **2007**, *129*, 12096–12097.

(8) Law, M.; Kind, H.; Messer, B.; Kim, F.; Yang, P. D. *Angew. Chem., Int. Ed.* **2002**, *41*, 2405–2408.

(9) Kolmakov, A.; Klenov, D. O.; Lilach, Y.; Stemmer, S.; Moskovits, M. *Nano Lett.* **2005**, *5*, 667–673.

(10) Kuang, Q.; Lao, C. S.; Wang, Z. L.; Xie, Z. X.; Zheng, L. S. *J. Am. Chem. Soc.* **2007**, *129*, 6070–6071.

(11) Zhang, D. H.; Liu, Z. Q.; Li, C.; Tang, T.; Liu, X. L.; Han, S.; Lei, B.; Zhou, C. W. *Nano Lett.* **2004**, *4*, 1919–1924.

(12) Law, M.; Kind, H.; Messer, B.; Kim, F.; Yang, P. D. *Angew. Chem., Int. Ed.* **2002**, *41*, 2405–2408.

(13) Maiti, A.; Rodriguez, J. A.; Law, M.; Kung, P.; McKinney, J. R.; Yang, P. D. *Nano Lett.* **2003**, *3*, 1025–1028.

(14) Garje, A. D.; Aiyer, R. C. *Int. J. Appl. Ceram. Technol.* **2007**, *4* (5), 446–452.

(15) Chen, X. H.; Mockovits, M. *Nano Lett.* **2007**, *7*, 807–812.

(16) Rani, S.; Roy, S. C.; Bhatnagar, M. C. *Sens. Actuators, B* **2007**, *122*, 204–210.

(17) Chowdhuri, A.; Sharma, P.; Gupta, V.; Sreenivas, K.; Rao, K. V. *J. Appl. Phys.* **2002**, *92*, 2172–2180.

(18) Jiao, Z.; Bian, L. F.; Liu, J. H.; Liu, J. H. *Mater. Res. Bull.* **2000**, *35*, 741–745.

11544 *J. Phys. Chem. C, Vol. 112, No. 30, 2008*

Kuang et al.

(19) Ansari, Z. A.; Ansari, S. G.; Ko, T.; Oh, J. H. *Sens. Actuators, B* **2002**, *87*, 105–114.

(20) Yu, J. H.; Choi, G. M. *Sens. Actuators, B* **1999**, *61*, 59–67.

(21) Ling, Z.; Leach, C.; Freer, R. *J. Eur. Ceram. Soc.* **2001**, *21*, 1977–1980.

(22) Qian, L. H.; Wang, K.; Li, Y.; Fang, H. T.; Lu, Q. H.; Ma, X. L. *Mater. Chem. Phys.* **2006**, *100*, 82–84.

(23) Dai, Z. R.; Pan, Z. W.; Wang, Z. L. *Adv. Mater.* **2003**, *13*, 9–24.

(24) Cheng, Y.; Xiong, P.; Fields, L.; Zheng, J. P.; Yang, R. S.; Wang, Z. L. *Appl. Phys. Lett.* **2006**, *89*, 093114.

(25) Liu, Z. Q.; Zhang, D. H.; Han, S.; Li, C.; Tang, T.; Jin, W.; Liu, X. L.; Lei, B.; Zhou, C. W. *Adv. Mater.* **2003**, *15*, 1754–1757.

(26) Heo, Y. W.; Kang, B. S.; Tien, L. C.; Norton, D. P.; Ren, F.; La Roche, J. R.; Pearton, S. J. *Appl. Phys. A: Mater. Sci. Process.* **2005**, *80*, 497–499.

(27) Suehiro, J.; Nakagawa, N.; Hidaka, S. I.; Ueda, M.; Imasaka, K.; Higashihata, M.; Okada, T.; Hara, M. *Nanotechnology* **2006**, *17*, 2567–2573.

(28) Wang, C.; Zhao, J. C.; Wang, X. M.; Mai, B. X.; Sheng, G. Y.; Peng, P.; Fu, J. M. *Appl. Catal., B* **2002**, *39*, 269–279.

(29) Zhang, M. L.; An, T. C.; Hu, X. H.; Wang, C.; Sheng, G. Y.; Fu, J. M. *Appl. Catal., A* **2004**, *260*, 215–222.

(30) Shen, Y. S.; Zhang, T. S. *Sens. Actuators, B* **1993**, *12*, 5–9.

(31) Wu, X. H.; Wang, Y. D.; Liu, H. L.; Li, Y. F.; Zhou, Z. L. *Mater. Lett.* **2002**, *56*, 732–736.

(32) Wagh, M. S.; Patil, L. A.; Seth, T.; Amalnerkar, D. P. *Mater. Chem. Phys.* **2004**, *84*, 228–233.

(33) Kim, K. W.; Cho, P. S.; Kim, S. J.; Lee, J. H.; Kang, C. Y.; Kim, J. S.; Yoon, S. J. *Sens. Actuators, B* **2007**, *123*, 318–324.

(34) Tien, L. C.; Norton, D. P.; Gila, B. P.; Pearton, S. J.; Wang, H. T.; Kang, B. S.; Ren, F. *Appl. Surf. Sci.* **2007**, *253*, 4748–4752.

(35) Martucci, A.; Buso, D.; De Monte, M.; Guglielmi, M.; Cantalini, C.; Sada, C. *J. Mater. Chem.* **2004**, *14*, 2889–2805.

(36) Cantalini, C.; Post, M.; Buso, D.; Guglielmi, A.; Martucci, A. *Sens. Actuators, B* **2005**, *108*, 184–192.

(37) Wang, D. S.; Xu, R.; Wang, X.; Li, Y. D. *Nanotechnology* **2006**, *17*, 979–983.

(38) Nokamura, Y.; Yoshioka, H.; Miyayama, M.; Yanagida, H.; Tsurutani, T.; Nakamura, Y. *J. Electrochem. Soc.* **1990**, *13*, 940–943.

(39) Jung, S. J.; Yanagida, H. *Sens. Actuators, B* **1996**, *37*, 55–60.

(40) Hu, Y.; Zhou, X. H.; Han, Q.; Cao, Q. X.; Huang, Y. X. *Mater. Sci. Eng., B* **2003**, *99*, 41–43.

(41) Tamki, J.; Shimanoe, K.; Yamada, Y.; Yamamoto, Y.; Miura, N.; Yamazoe, N. *Sens. Actuators, B* **1998**, *49*, 121–125.

(42) Hidalgo, P.; Castro, R. H. R.; Coelho, A. C. V.; Gouvea, D. *Chem. Mater.* **2005**, *17*, 4149–4153.

(43) Jain, K.; Pant, R. P.; Lakshmikumar, S. T. *Sens. Actuators, B* **2006**, *113*, 823–829.